

Renormalization group analysis of graphene-phosphorene van der Waals heterostructure with spin-wave dependent response function

Sushant Kumar Behera and Pritam Deb*

Advanced Functional Material Laboratory (AFML), Department of Physics, Tezpur University (Central University), Tezpur-784028, India.

*Corresponding author

Email address: pdeb@tezu.ernet.in (Pritam Deb)

Abstract:

Weak-coupling phenomena of the two-dimensional (2D) Hubbard model is gaining momentum as a new interesting research field due to its extraordinarily rich behavior as a function of the carrier density and model parameters. Thus, there is a rapidly growing interest in the transmission of information encoded by electron and atomic spins which, in principle, can be realized by the propagation of spin waves through low-dimensional sheets. In this paper, we demonstrate the spin-wave dependent electronic structure and susceptibility behavior of model 2D graphene-phosphorene van der Waals (vdW) heterostructure in the framework of density functional theory simulations combining renormalization group (RG) approach. We implement Aharonov-Bohm-Coulomb-Dirac (ABCD) formulated field-theoretic approach for the weakly interacting Fermi system with nearest-neighbor hopping amplitudes. The analytical approach is further extended for spin-wave dependent susceptibility behavior.

Keywords: Renormalization group (RG) theory; two dimensional (2D) van der Waals (vdW) heterostructure; weakly interacting Fermi system; spin-wave dependent susceptibility; Vertex response function

1. Introduction

Atomically thin two dimensional (2D) materials, like h-BN, graphene and its family, TMDCs, black phosphorous, etc. cover interesting field of research because of their rich mechanical¹⁻³, electronic^{4,5}, optical^{6,7} and electrochemical assets with an extensive variety of promising applications⁸⁻¹⁰. Concerning beyond the field of 2D atomic crystals, isolated 2D atomic planes can be reassembled layer by layer in a precisely chosen sequence to form heterostructures, known as 2D van der Waals (vdWs) heterostructure prevailing interesting and new properties¹¹. In recent times, multilayer vdWs heterostructures, chemically different 2D structures, have attracted the primary research attention unlike monolayer pristine systems, like Grp/h-BN¹², Grp/TMDC¹³, h-BN/TMDC¹⁴, Grp/Silicene¹⁵ and TMDC/TMDC¹⁶. While, many 2D materials (e.g. graphene and MoS₂) with efficient carrier mobilities (i.e. high *on-off* ratio)^{17,18} restrict their nano-dimension heterolayer device applications. In this case, strong transport is essential to

inoculate the perturbations present at defected edge sites. As a result, the transport behaviour can be modulated via electric field or gate voltage for the desired field-effect transmission. These layered 2D vdW heterostructures possess superior efficiency for carrier inoculation via barrier height modulation¹⁹. In this regard, phosphorene (P), a puckered honeycomb 2D material, possesses fascinating electronic and optical properties, such as finite direct band gap (~ 1.5 eV at monolayer) and high mobility (10^3 cm²V⁻¹s⁻¹ at 300 K) due to its structural anisotropy²⁰⁻²⁴. Notably, P based field-effect transistors (FETs) and high-frequency nano-electromechanical resonators have been validated in recent past. Moreover, phosphorene shows a giant phononic anisotropy, which is squarely reverse compared to its electronic counterpart, supporting the asymmetrical transport of electronic/holes and phonons in heterostructure form with graphene²⁵. To analyze prototypic 2D model for the electronic degrees of freedom, Hubbard model including Renormalization Group (RG) theory is promising in case of 2D planes²⁶. In particular, 2D Hubbard model is appropriate to explain attracting phenomena of weakly interacting systems which can be tuned by their carrier density. Besides, large scale numerical algorithms are worked out to solve such 2D interacting Hubbard models including related model parameters²⁷. In such systems, weak interaction reveals antiferromagnetic ground state close to half-filling and symmetric s-wave phase away from half-filling region. In such cases, conventional perturbation theory fails at a certain region close to the half-filling region, where challenging and frequent infrared deviations raise due to weakly interacting Fermion system²⁸⁻³⁰ and van Hove singularities³¹ including the Aharonov-Bohm (AB) potential field for 2D graphene monolayer system³²⁻³⁴. Moreover, theoretical model of 2D weakly interacting Fermi systems having challenging singularities near weakly interacting region is still lacking in the current analytical prospects for vdW heterostructures. Thus, RG theory is presently the most promising and well-ordered technique for such 2D weakly interacting Fermi systems^{35,36}.

In the present manuscript, we implement RG theory to the 2D Hubbard model of Graphene-Phosphorene (Grp-P) heterostructure considering nearest neighbor hopping amplitudes of dense electron distribution profile close to half-filling region. Here, we particularly calculate the trend of collective two particle couplings in a single loop stage, completely ignoring the inappropriate energy and linear momentum dependency, but considering vital tangential momentum dependency being a dynamic parameter. We further extend the RG theory to obtain the susceptibility values to analyze the physical response of uncertainties gestured by diverging couplings in weakly interacting vdW heterostructure. Charge-density, spin-density and singlet function based susceptibilities have been considered during analytical calculations at various pairing symmetries. Here, spin-density phase diagram has been presented close to half-filling

region of this 2D Hubbard model. The obtained results show the critical energy scale behavior away from the half-filling region with perfect nesting. Moreover, the analytical results have been corroborated with the first principle based density functional simulations. Considering both the analytical and simulation results, field-effect transmission probability has been investigated as a consequence of response functions targeting to develop the prototype of a dual-gate FET (DG-FET).

2. Methodology

2D Hubbard model is the simplest class of models describing electrons moving on a lattice with weak electron-electron interactions. However, electron-electron interactions can break one or more symmetries of the Hamiltonian, and this leads to phases such as antiferromagnetism, charge or density of spin-waves, etc. In this regard, RG theory is presently the most promising and best controlled approach to low dimensional systems with competing singularities at weak coupling region via Aharonov-Bohm (AB) field potential. Here, direct device application through AB field potential is unrealistic in pristine monolayer form, until and unless corroborated with vdW multilayer heterosystem using *ab initio* pseudopotential simulation. Thus, we have implemented AB field theoretic approach, unlike Dirac-like field theory. We use the field theoretic approach to frame the RG formulation for the 2D Fermi systems via vertex response functions.

2.1. Field Theory Framework

The Hamiltonian with the order of second quantization (H_{SQ})³⁷ unfolding the massless 2D Dirac fermions is cited below, as

$$H_{SQ} = \int d\nu \xi^\dagger(\nu) \{v_F [-i\hbar \partial_t - \sigma \cdot \nabla - eV(\nu)] \xi(\nu) \} \quad (1)$$

where ‘e’, ‘ σ ’, ‘ v_F ’ and ‘ ξ^\dagger ’ are the electron charge, spin-wave projection, Fermi velocity and Grassmann variable, respectively. The Coulomb field potential originated due to the net charge of ‘Ze’ positioned at the origin is $V(\nu) = \frac{Ze}{4\pi\epsilon_0\nu}$, similarly the AB field solenoid aligned at the

same point provides $A(\nu) = \frac{\Phi}{2\pi} \left(-\frac{y}{\nu^2}, \frac{x}{\nu^2}\right)$ with a fixed total magnetic flux of Φ . Being the fixed magnetic flux, Pearl’s substitution approach is limited in the flow equation. This establishes the Aharonov-Bohm-Coulomb-Dirac (ABCD) field problem in the present model 2D vdW heterosystem³⁸.

The partial wave expansion of the equation (1) can be further expanded using rotational symmetry as follow,

$$\xi(r) = \sum_{j=-\infty}^{j=+\infty} \begin{pmatrix} e^{i(j-\frac{1}{2})\theta} & 0 \\ 0 & ie^{i(j+\frac{1}{2})\theta} \end{pmatrix} e^{-i\frac{\pi}{4}\sigma_1} \frac{\xi_j(\nu)}{\sqrt{2\pi\nu}} \quad (2)$$

which decouples the system Hamiltonian into diverse partial-wave sectors as given below

$$H_S = \hbar \sum_{j=-\infty}^{j=+\infty} d\nu \xi_j^\dagger(\nu) (-i\partial_\nu \sigma_3 - \frac{C}{\nu} \sigma_0 + \frac{j+\phi}{\nu} \sigma_1) \xi_j(\nu) \quad (3)$$

Here, $j = \pm 1/3, \pm 3/2, \dots$ is the net angular momentum and we consider the dimension-free

Coulomb field coupling, $C = \frac{Ze^2}{4\pi\epsilon_0\hbar}$. Apart from the kinetic term, each radical Hamiltonian in

Eqn. (3) contains the Coulomb field potential and the centrifugal field potential, both of them possess scale-invariant form (i.e. $1/\nu$). Most interesting physical quantities are the charge density $\rho(\nu) = -e \langle \xi^\dagger(\nu) \xi(\nu) \rangle$ and current density $J(\nu) = -e\nu_F \langle \xi^\dagger(\nu) \sigma \xi(\nu) \rangle$ in the ground state of the ABCD Hamiltonian Equation (1). The corresponding coupling presents scattering amplitude located at potential center and corresponding energy dependency is to be obtained using RG equations.

2.2. Renormalization Group Theory

We have taken weakly interacting spin-half Fermions with single-particle basis state with crystal momentum (k_c), *up or down* spin-wave projection, $\sigma \in \{\uparrow, \downarrow\}$ and kinetic energy (E_K). Thus, the behavioral aspects of the system can be determined via following flow Equation,

$$S[\xi, \bar{\xi}] = \sum_K (if_0 - \xi_k) \bar{\xi}_K \xi_K - \gamma[\xi, \bar{\xi}] \quad (4)$$

where, $K = (f_0, k, \sigma)$ presents a multi index parameter connecting the frequency (f_0) with each particle quantum numbers; Grassmann variables (ξ_k and $\bar{\xi}_k$) are allied to the formation and extinction operators, $\xi_k = \varepsilon_k - \mu$ is the energy related to a particle depending on the chemical potential (μ) and $\gamma[\xi, \bar{\xi}]$ is a random many body coupling factor [39, 40]. Here, all the connected flow equations via Green functions can be achieved from the functional which is used for their generation, given below

$$G[\eta, \bar{\eta}] = \log \left\{ \int \partial\mu_c[\xi, \bar{\xi}] e^{-\gamma[\xi, \bar{\xi}]} e^{(\bar{\xi}, \eta) + (\bar{\eta}, \xi)} \right\} \quad (5)$$

with the normalized Gaussian measure.

The infinite hierarchy in flow equations is essential to check at a single-loop level to predict dominant structural uncertainties in the vdW system within weakly interacting limit, neglecting other irrelevant components of the effective interactions. Moreover, energy corrections of each iteration step are confined to one-particle vertex function (Γ) and used for further calculations. The spin-wave structure of Γ can be used for a spin rotation invariant system with response flow equation, which is given as follow,

$$\Gamma(K'_1, K'_2; K_1, K_2) = [\Gamma_s(k'_1, k'_2; k_1, k_2) \Lambda^{1/2} S_{\sigma'_1, \sigma'_2; \sigma_1, \sigma_2} + \Gamma_t(k'_1, k'_2; k_1, k_2) \Lambda^{3/2} T_{\sigma'_1, \sigma'_2; \sigma_1, \sigma_2}] \quad (6)$$

where, K_1 and K_2 present the multi indexed particle quantum numbers for both spin arrangements, singlet ($S_{\sigma'_1, \sigma'_2; \sigma_1, \sigma_2} = \frac{1}{2}(\delta_{\sigma'_1 \sigma_1} \delta_{\sigma'_2 \sigma_2} - \delta_{\sigma'_1 \sigma_2} \delta_{\sigma'_2 \sigma_1})$) and triplet ($T_{\sigma'_1, \sigma'_2; \sigma_1, \sigma_2} = \frac{1}{2}(\delta_{\sigma'_1 \sigma_1} \delta_{\sigma'_2 \sigma_2} + \delta_{\sigma'_1 \sigma_2} \delta_{\sigma'_2 \sigma_1})$) projection operators are used for two particle spin space, Λ is the energy scale varying at a fractional trend for singlet and triplet operators.

We extend the RG equations to obtain linear response behaviour (i.e. spin-wave susceptibility value) of the system towards finite applied external electric field^{41, 42}. Finite external field (F_E) leads to an additional contribution to the action of the flow equation, which is given as follow

$$\zeta[F_E; \xi, \bar{\xi}] = -\sum_q [\bar{F}_E(q) \Phi(q) + F_E(q) \bar{\Phi}(q)] \quad (7)$$

Here, Grassmann variables in bilinear form ($\Phi(q)$), Hermitian conjugate ($\bar{\Phi}(q)$) and $\bar{F}_E(q)$ is the complex conjugate of $F_E(q)$. We have calculated the response of the field interaction towards

electronic charge density, $\rho(q) = \sum_{k, \sigma} \bar{\xi}_{k-q, \sigma} \xi_{k, \sigma}$ and z-direction dependent spin density,

$s^z(q) = \sum_k [\bar{\xi}_{k-q, \uparrow} \xi_{k, \uparrow} - \bar{\xi}_{k-q, \downarrow} \xi_{k, \downarrow}]$ and response to coupling fields which interacts with the change

in singlet operator, $\Delta(q) = \sum_{k, \sigma} \sigma \hat{\partial}(k) \xi_{k+q, \sigma} \xi_{-k, -\sigma}$, where $\hat{\partial}(k)$ is an even parity function satisfying

the orbital symmetry of the coupling operator (i.e. s wave). The linear response of the

expectation value $\theta(q) = \zeta^{-1} \langle \Phi(q) \rangle = \frac{1}{\gamma} \frac{\partial \log[F_E]}{\partial \bar{F}_E(q)}$ with the flow equation of the partition

function

$$[F_E] = \int d\mu_C[\xi, \bar{\xi}] e^{-\zeta[\xi, \bar{\xi}] - \zeta'[F_E; \xi, \bar{\xi}]} \quad (8)$$

where the susceptibility follows like,

$$\chi(q) = \left. \frac{\partial \theta(q)}{\partial F_E(q)} \right|_{F_E=0} = \zeta^{-1} \langle \Phi(q) \bar{\Phi}(q) \rangle \Big|_{F_E=0} \quad (9)$$

Here, translation and spin rotation invariant systems are considered with conserved charge in the absence of an external field (F_E). Here, in such normal and non-symmetrical broken phase, $\langle \Phi(q) \rangle$, the expectation value nullifies at $F_E(q) \rightarrow 0$.

3. Results and Discussions

3.1. Vertex function Findings

The flow of the vertex function (Γ) and the susceptibility (χ) values have been calculated analytically using RG theory for several choices of the bare interaction, termed as the AB field potential ($U > 0$), the next nearest neighbor hopping amplitude ($t < 0$) and the chemical potential (μ), where t and μ have been fixed so that the Fermi surface and particle density are approaching to ε_k and half-filling (i.e. $n \approx 1$, $|\mu| \rightarrow 0$), respectively. Momentum dependent flow of the vertex functions are obtained for the three considered systems at low dimensional scale. It is observed that the flow of the vertex function achieves a density value ($n \approx 0.992$), i.e. close to half-filling region at $t=0$ and $|\mu|=0.005$ (plotted in Figure 1(a)). Here, the singlet part of the vertex function is taken at specified values of momenta on the Fermi surface including the values of momenta, where strong renormalization of Γ occurs. Most probably, the singlet vertex function possesses its leading values supporting *umklapp scattering* along the diagonal direction of the k -space Brillouin zone. It is observed from the RG theory calculation that the density decreases away from half-filling (i.e. $n \approx 1$, $|\mu| \rightarrow 0$) region in a step-like manner and the calculations fail into a region, where s -wave symmetry dominates with pairing correlations at necessarily low scale energy levels indicating quantum confinement (i.e. nanostructuring) in the *Grp-P* heterostructure system.

Two types of antiferromagnetic spin-wave (*incommensurate* and *commensurate*) susceptibilities have been obtained from the numerical calculations to validate the physical instability associated with the diverging vertex function as a consequence of response functions⁴⁶⁻⁴⁹. It is observed that the *incommensurate* spin susceptibilities can be neglected compared to their respective *commensurate* counterparts (shown in Figure 1(b)) due to the incommensurability parameter ($\delta \rightarrow 0$) nearing to half-filling ($n \approx 1$, $|\mu| \rightarrow 0$) as a function of energy scale. Moreover, the ratios between the two susceptibility values of monolayer system in case of weakly interacting s -wave region are in the same scale, whereas the ratios of free susceptibility are much reduced indicating the validity of response functions for 2D weakly coupled Fermi systems. In addition, the ratio in case of hetero bilayer is much greater compared to its monolayer system. Thus, antiferromagnetic wave vector based spin-wave susceptibility dominates over coupled

susceptibilities at low scale energy level (i.e. *ground state*), confirming the existence of antiferromagnetic ground state with rotational spin invariance.

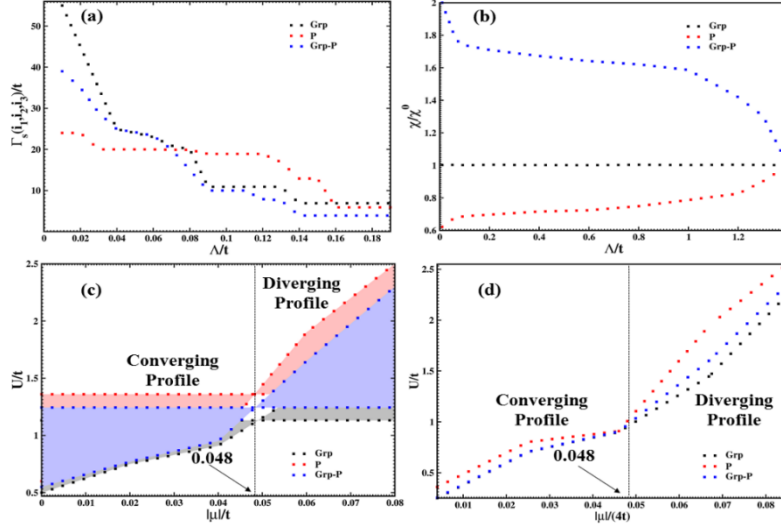


Figure 1. (a) Flow of the singlet vertex function, Γ , as a function of Λ for several selections of momenta values, k_{F1} , k_{F2} and k_{F3} . (b) The flow of the ratio of weakly interacting and free susceptibility values depending on Λ values for the three systems. The model parameters are $U=t$ and $t=0$, and the chemical potential $|\mu|=0.005$. (c) The (μ, U) phase diagram for $t=0$ close to half-filling ($n=1$, $|\mu| \rightarrow 0$) region; the solid line represents the spin-density-wave regime. (d) The (t, U) phase diagram for $4t < 0$ value below the half-filling ($|\mu| < 0$) region; the dotted lines represent the spin-density-wave regime.

We show the phase diagram of μ and U at half-filling measured by the prevailing uncertainty from the flow equation (shown in Figure 1 (c)). The leading uncertainty region in case of *commensurate* spin-wave density is detached from the *s*-wave coupling region via a narrow strip where *incommensurate* spin-wave density fluctuations show dominant effect with $q=(\pi, \pi-\delta)$. For small value of U , the region surrounding half-filling is exponentially small, where uncertainties in spin-wave density play a dominant effect. The value of (t, U) , *in-plane* phase diagram is shown in Figure 1 (d) with $|\mu|=4t$ and $\mu < 0$ (below half-filling). It is observed that the chemical potential is fixed at the van Hove singularity⁵⁰ irrespective of the value of spin-wave density, which is decreasing away from half-filling region with growing value of $|\mu|$ at 0.048, one critical point in the flow equation.

The behavioral trend of critical energy scale, Λ_c , depending on the function at $t < 0$ where, $|\mu| \rightarrow 0$ and $U=t$ is plotted in Figure 2 (a). The shrinkage in the value of Λ_c with growing trend of $|\mu|$ confirms that the E_F residues on the van Hove singularity within the weakly interacting regime having only Fermi surface nesting dominance. Momentum variables of Γ have been projected upon the Fermi surfaces at specific points, where the strong renormalization of the vertex function occurs. Here, total 8 fixed points considered for the normalization process. Besides, additional 8 points have been considered in a more refined projection scheme upon the van Hove surface to check the collective effect. As a result, sum total 16 points (8 for Fermi surface and 8 for van Hove surface) have been taken during the flow equation calculations. These refinements, in the response function of the spin-wave density scheme, enhance the analytical calculation efficiency significantly with a reasonable reduction in critical energy scale, without altering Γ and χ values, qualitatively. The variation trend of Λ_c as a function of the inverse number of discretization points, N_0 , upon the Fermi surface at fixed choice of model parameters is shown in Figure 2(b). It is noticed that the critical energy scale is varying in a discrete manner with 8 discretization points, and resumes stability for next 8 points with right order of magnitude indicating the controlled trend of flow equation for weakly interacting systems.

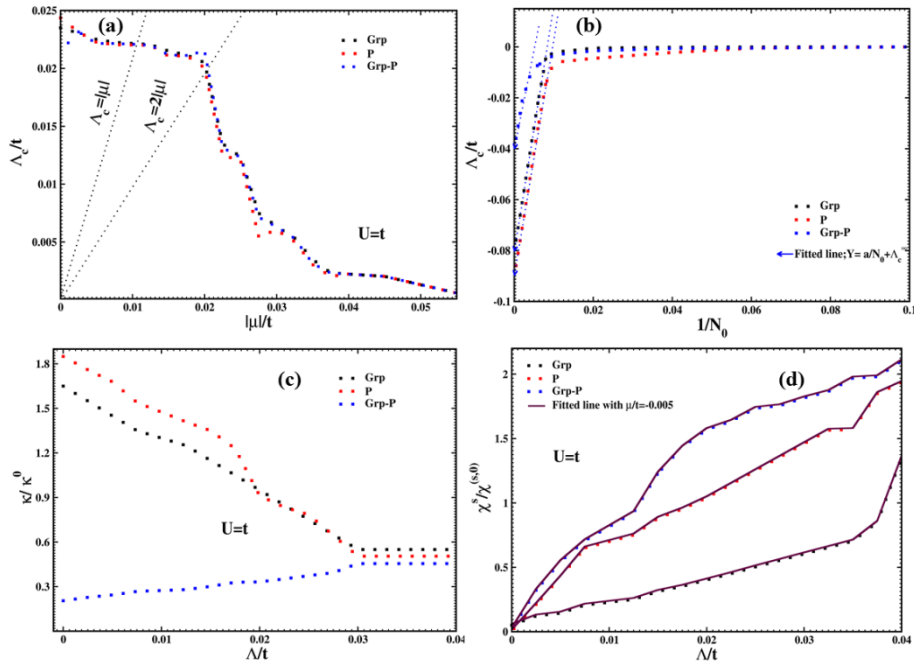


Figure 2. The critical energy scale, Λ_c , as a function of (a) μ at $U=t$ and $n=1$. The dotted black lines present the functions for $\Lambda_c = |\mu|$ and $\Lambda_c = 2|\mu|$. (b) number of discretization points, N_0 , upon Fermi surface at $U=t$, $n=1$ and $|\mu| = 0.005$. The dotted black lines represent the functions $Y = a/(N_0 + \Lambda_c)$. The flow of (c) compressibility, κ , and (d) homogeneous spin susceptibility as a function of Λ at fixed value of $|\mu| = 0.005$ for $U = t$ and $n=1$.

The values of compressibility and homogeneous spin susceptibility have been calculated depending on the energy scale (shown in Figure 2(c) and (d)), respectively for the three systems. These two parameters can be realized directly from the forward scattering of vertex function via Landau equations of Fermi-liquid theory⁵¹. The free compressibility, k^0 , and spin-wave susceptibility, $\chi^{(s, 0)}$, are refined ignoring infrared cut-off values as per the Fermi-Liquid theory. As a result, the flow equations of the vertex response function is entirely because of the flow of the Landau functions at the initial stage of the normal random phase approximation of the Hubbard model at critical energy scale value, $\Lambda=\Lambda_0$. The compressibility is inhibited at low scale energy levels close to half-filling region, which is expected for systems having a finite bandgap near to ‘ μ ’, with dominant uncertainty in spin-wave density. Besides, the values of the compressibility diverge with respect to the reduction in homogeneous spin-wave susceptibility values away from half-filling region, where s -wave uncertainties play major role acting indicating a finite spin-wave bandgap opening trend in any singlet or triplet spin-wave 2D Fermi systems⁵². It is found that the spin-wave susceptibility flows from zero to negative values which implies that our single loop calculation fails, when it reaches strongly interacting regime. This trend is validated only in weakly interacting region applied for 2D Fermi system. Thus, one diverging compressibility is found mentioning a strong tendency toward phase transition and separation. As a result, the increase of k sets is very close to the uncertainty, where the renormalized interactions achieve large value that the single loop findings are not further validated. The stability is prominent at higher energy scales (i.e. $0.04 \leq \frac{\Lambda}{t} \leq 0.03$) from the plot in figure 2((c) and (d)). Moreover, we have shown the trend of free susceptibilities (χ^0) at specific choice of t and μ values (shown in supplementary information Figures S1) which is strongly supporting the trend of homogeneous spin-wave susceptibility.

4. Conclusion

A study on the spin-wave response function behavior of vdW Grp-P heterostructure based DG-FET was presented via field-theory perspective implementing analytical and *ab initio* quantum mechanical simulations. This formulation can be used systematically to identify coupling uncertainties in 2D weakly interacting Fermi systems. In this system, critical energy can be scaled at specific singular points where vertex functions and susceptibilities diverge and become finite. Moreover, the instabilities are modulated via short range antiferromagnetic correlations present in the system, which is noticed from the flow of vertex functions and susceptibilities. This antiferromagnetic ordering is retained in the ground state of such 2D systems accompanied with rotational spin invariance. The analytical results show an unusual singularity of van Hove

kind in 2D heterostructure. This finding supports room temperature stability and on-state modeling of the system for electronic devices in future.

Conflicts of interest

There are no conflicts to declare.

ACKNOWLEDGEMENTS

S.K.B. acknowledges Department of Science & Technology (DST), Government of India for providing financial support in terms of INSPIRE Fellowship (IF150325). The authors would like to thank Tezpur University for providing High Performing Cluster Computing (HPCC) facility.

References

1. K. S. Novoselov et al, *Science*, 2004, **306**, 666.
2. T. Georgiou et al, *Nat. Nanotechnol.*, 2013, **8**, 100103.
3. A. K. Geim et al, *Science*, 2009, **324**, 1530.
4. Y. Cai, G. Zhang and Y. -W. Zhang, *J. Am. Chem. Soc.*, 2014, **136**, 6269.
5. K. Novoselov et al, *Nature*, 2005, **438**, 197.
6. S. Qian, X. Sheng, X. Xu, Y. Wu, N. Lu, Z. Qin, J. Wang, C. Zhang, E. Feng, W. Huanga and Y. Zhou, *J. Mater. Chem. C*, 2019,**7**, 3569.
7. K. Lai, H. Li, Y. -K. Xu, W. -B. Zhang and J. Dai, *Phys. Chem. Chem. Phys.*, 2019, **21**, 2619-2627.
8. Y. -C. Rao, S. Yu and X. -M. Duan, *Phys. Chem. Chem. Phys.*, 2017,**19**, 17250-17255.
9. X. Zhou, F. Li, Y. Xing and W. Feng, *J. Mater. Chem. C*, 2019,**7**, 3360.
10. S. K. Behera and P. Deb, *Phys. Chem. Chem. Phys.*, 2018, **20**(41), 26688.
11. A. K. Geim and I. V. Grigorieva, *Nature*, 2013, **499**, 419.
12. S. K. Behera and P. Deb, *RSC Advances*, 2017, **7**(50), 31393.
13. S. K. Behera, P. Deb and A. Ghosh, *ChemistrySelect*, 2017, **2**(13), 3657.
14. Z. Huang et al, *J. Phys. D: Appl. Phys.*, 2014, **47**, 075301.
15. M. F. Bhopal, D. W. Lee, A. ur Rehman and S. H. Lee, *J. Mater. Chem. C*, 2017, **5**, 10701.
16. A. Hjorth Larsen et al, *J. Phys.: Condens. Matter*, 2017, **29**, 273002.
17. F. Schwierz et al, *Nat. Nanotechnol.*, 2010, **5**, 487.
18. B. Radisavljevic et al, *Nat. Nanotechnol.*, 2011, **6**, 147.
19. C. Yongqing, G. Zhang and Y. -W. Zhang, *J. Phys. Chem. C*, 2015, **119**, 13929.
20. J. L. Lado and J. Fernández-Rossier, *2D Mater.*, 2017, **4**, 035002.
21. J. Yuan et al, *ACS Nano*, 2015, **9**, 555.
22. H. Liu et al, *ACS Nano*, 2014, **8**, 4033.
23. L. Li et al, *Nat. Nanotechnol.*, 2014, **9**, 372.

24. M. Talukdar, S. K. Behera, K. Bhattacharya and P. Deb, *Appl. Surf. Sci.*, 2019, **473**, 275.
25. Y. Shi et al, *Nano Lett.*, 2012, **12**, 2784.
26. Y. Hadad and B. Z. Steinberg, *Phys. Rev. Lett.* 2010, **105**, 233904.
27. B. Liu et al, *Adv. Mater.*, 2015, **27**, 4423.
28. D. Torelli and T. Olsen, *2D Mater.*, 2019, **6**, 015028.
29. K. G. Wilson, *Rev. Mod. Phys.* 1975, **47**, 773.
30. R. Shankar, *Rev. Mod. Phys.* 1994, **66**, 129.
31. N. E. Bickers, D. J. Scalapino and S. R. White, *Phys. Rev. Lett.*, 1989, **62**, 961.
32. O. Y. Yermakov et al, *Phys. Rev. B*, 2015, **91**, 235423.
33. A. Kumar et al, *Nano Lett.*, 2015, **15**, 3172.
34. D. Ebert, V. C. Zhukovsky and E. A. Stepanov, *J. Phys.: Condens. Matter*, 2014, **26**, 125502.
35. N. Furukawa, T. M. Rice and M. Salmhofer, *Phys. Rev. Lett.*, 1998, **81**, 3195.
36. M. Salmhofer, *Commun. Math. Phys.*, 1998, **194**, 249.
37. J. W. Negele and H. Orland, Quantum Many Particle Systems. 1987, *Addison-Wesley* Reading MA.
38. M. O. Goerbig, *Rev. Mod. Phys.*, 2011, **83**, 1193.
39. Y. Aharonov and D. Bohm, *Phys. Rev.*, 1959, **115**, 485.
40. B. J. Dalton, J. Jeffers and S. M. Barnett, *Annals of Physics*, 2016, **370**, 12.
41. M. Zhu, M. B. Shalom, A. Mishchenko, V. Fal'ko, K. Novoselov and A. Geim, *Nanoscale*, 2018, **10**, 3020.
42. K. E. Newman and E. K. Riedel, *Phys. Rev. B*, 1982, **25**, 264.
43. P. Giannozzi et al, *J Phys: Conden. Matter*, 2009, **21**(39), 395502.
44. P. E. Blöch, *Phys. Rev. B*, 1994, **50**, 17953.
45. H. J. Monkhorst and J. Pack, *Phys. Rev. B*, 1976, **13**, 5188.
46. M. K. Chan et al, *Nat Commun.*, 2016, **7**, 10819.
47. T. E. Mason et al, *Phys. Rev. Lett.*, 1992, **68**, 1414.
48. S. A. Kivelson et al, *Rev. Mod. Phys.*, 2003, **75**, 1201.
49. S. Higashitani, *Phys. Rev. B*, 2014, **89**, 184505.
50. R. Žitko, J. Bonča and T. Pruschke, *Phys. Rev. B*, 2009, **80**, 245112.
51. G. Y. Chitov and D. Sénéchal, *Phys. Rev. B*, 1998, **57**, 1444.
52. V. B. Shenoy, *Phys. Rev. A*, 2013, **88**, 033609.

Supplementary Information

In Figure S1, we have shown the Free Susceptibilities variation with respect to flow equation of the system [1-5].

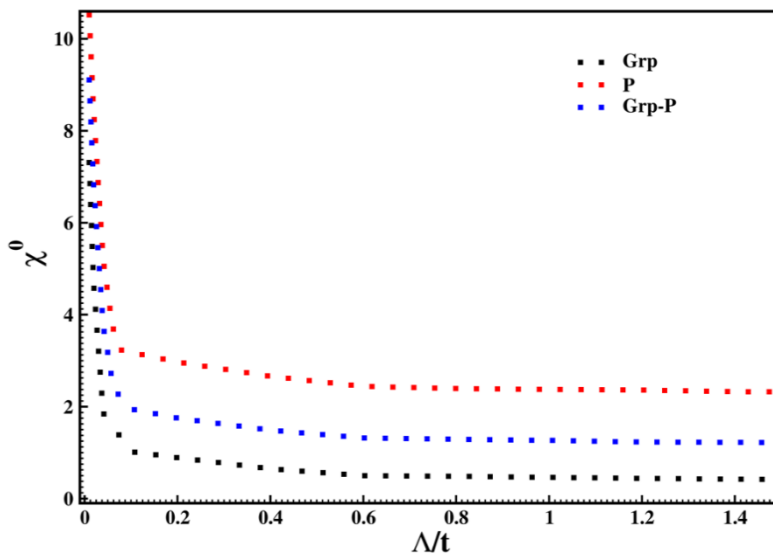


Figure S1. Free (non-interacting) susceptibilities of graphene monolayer, phosphorene monolayer and graphene-phosphorene bilayer for $t=0$ and $|\mu|= 0.005$.

References

1. S. Datta, *Phys. Rev. B*, 1992, **45**(3), 1347.
2. E. R. Davidson, *J. Comput. Phys.*, 1975, **17**, 87.
3. F. T. Parker et al, *Phys. Rev. B*, 1993, **47**, 7885.
4. G. R. Blake et al, *Phys. Rev. B*, 2002, **65**, 174112.
5. R. Winpenny, 2011 Molecular Cluster Magnets. *World Scientific*, 2011, ISBN 9789814322942, p.119.